Bioconjugate Chemistry

Article

pubs.acs.org/bc

Functionalized Layered Double Hydroxide Nanoparticles Conjugated with Disulfide-Linked Polycation Brushes for Advanced Gene Delivery

H. Hu, K. M. Xiu, S. L. Xu, W. T. Yang, and F. J. Xu*

State Key Laboratory of Chemical Resource Engineering, Key Laboratory of Carbon Fiber and Functional Polymers, Ministry of Education, College of Materials Science and Engineering, Beijing University of Chemical Technology, Beijing 100029, China

ABSTRACT: Layered double hydroxides (LDHs) have aroused great attention as potential nanosized drug delivery carriers, but independent inorganic LDH wrapped with DNA shows very low transfection efficiency. To manipulate and control the surface properties of LDH nanoparticles is of crucial importance in the designing of LDH-based drug carriers. In this work, surface-initiated atom transfer radical polymerization (ATRP) of 2-(dimethylamino)-ethyl methacrylate (DMAEMA) is employed to tailor the functionality of LDH surfaces in a well-controlled manner and produce a series of well-defined novel gene delivery vectors (termed as LDH-PDs), where a flexible three-step method was first developed to introduce the ATRP initiation sites containing disulfide bonds onto LDH surfaces. In comparison the pristine LDH particles, the resultant LDH-PDs exhibited better ability to condense plasmid DNA (pDNA) and much higher levels to delivery genes in different cell lines including COS7 and HepG2 cell lines. Moreover, the LDH-PDs also could largely enhance cellular uptake. This present study demonstrates that functionalization of bioinorganic LDH with flexible polycation brushes is an effective means to produce new LDH-based gene delivery systems.

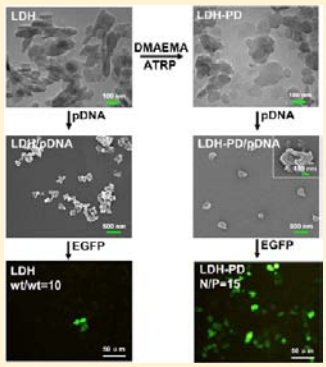

INTRODUCTION

The key of gene therapy is to design gene delivery vectors with low cytotoxicity and high transfection efficiency.[1,2] Recently, some advances have been achieved in the application of nanomaterials, especially inorganic nanoparticles, as drug and gene delivery carriers.[3,4] Layered double hydroxides (LDHs), also known as anion host−guest-layered nanoparticles, have been widely investigated as effective materials for biomedical applications, due to their ease of preparation, low cost, good biocompatibility, low cytotoxicity, high drug loadings, and good interaction with biomolecules.[5−11] LDH is represented by the general formula $[M_{1-x}^{II}M_x^{III}(OH)_2][A_{x/m}^{m-}\ nH_2O]$ (abbreviated notation $M_R^{II}M^{III}/A$ with $R = (1 - x)/x$), where M^{II} represents a divalent metal cation, M^{III} a trivalent metal cation and A^{m-} an anion of any type.[12] Exchangeable anions located in interlayer spaces compensate for positive charge of brucite-type layer. Most negatively charged biomolecules can be incorporated into LDHs.[10,13−17] DNA plasmids could interact with or intercalate into LDH nanoparticles, indicating that LDH is a potential inorganic matrix for gene delivery.[10] However, the low transfection efficiency mediated by LDH needs to be further improved.

The ability to manipulate and control the surface properties of a biomaterial is of crucial importance in designing new biomedical materials.[18,19] Further improvements of LDH surface properties can be accomplished via coupling functional molecules, such as cancer-cell targeting ligands.[14−18] Covalent tethering of well-defined polymer chains on a solid substrate is an effective method for modifying the surface properties.[19] Rich hydroxyl-exposed LDH surfaces could be derivatized to serve as initiation sites for further improvements via coupling functional molecules.[11] It has been demonstrated that well-defined cationic poly((2-dimethylamino)ethyl methacrylate) (or P(DMAEMA)) can spontaneously condense negatively charged DNA into compact nanocomplexes, protect plasmid DNA from enzymatic degradation by nucleases, and facilitate cellular transfection.[20] It would be ideal if LDH surfaces can be functionalized with well-defined P(DMAEMA) brushes to produce new LDH-based gene vectors.

In our work, surface-initiated atom transfer radical polymerization (ATRP) of DMAEMA was employed to tailor the functionality of LDH surfaces in a well-controlled manner and produce a series of well-defined organic−inorganic hybrids (termed as LDH-PDs). ATRP is a recently developed 'controlled' radical polymerization method.[21] A flexible three-step method was first developed to introduce the ATRP initiation sites containing disulfide bonds onto LDH surfaces (Scheme 1). Well-defined cationic LDH-PDs consisting of LDH and disulfide-linked cationic P(DMAEMA) brushes were subsequently prepared via ATRP. The LDH-PD hybrids were expected to provide much flexibility to condense pDNA with suitable particle sizes and mediate efficient gene transfection. The LDH-PD nanoparticles were characterized by X-ray photoelectron spectroscopy (XPS), thermal gravimetric analysis (TGA), and transmission electron microscopy (TEM), respectively.

Received: December 21, 2012
Revised: May 18, 2013
Published: May 20, 2013

Scheme 1. Schematic Diagram Illustrating the Preparation Processes of P(DMAEMA)-Graft-LDH Hybrids via ATRP

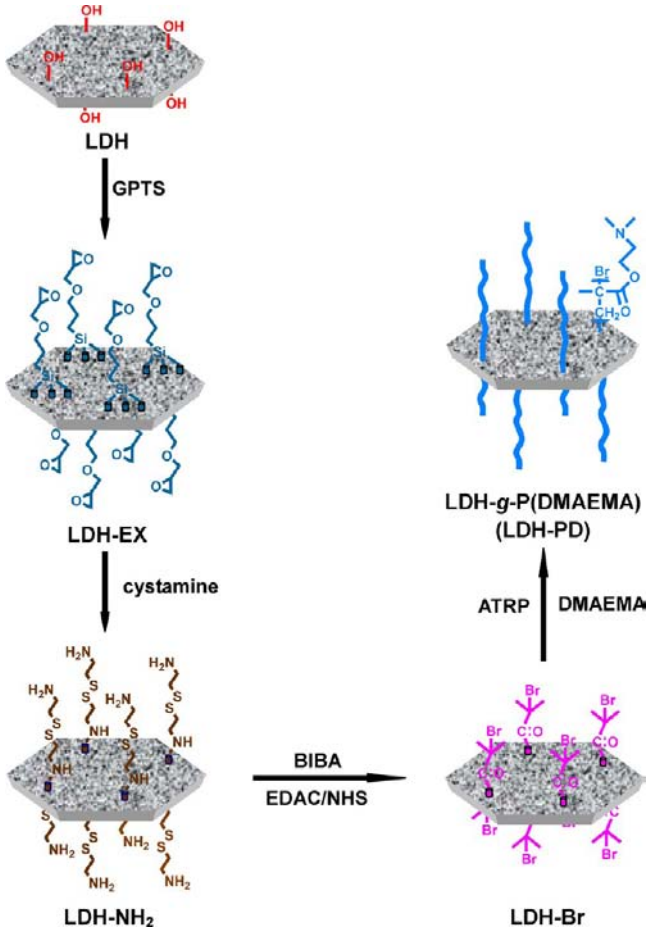

The gene transfer abilities of these LDH-based vectors were investigated in detail through a series of experiments.

EXPERIMENTAL PROCEDURES

Materials. Layered double hydroxide (LDH), 3-(glycidoxypropyl)triethoxysilane (GPTS), cystamine dihydrochloride (>98%), branched polyethylenimine (PEI, M_w ~25000 Da), 1-ethyl-3-(3-dimethylaminopropyl)carbodiimide hydrochloride (EDAC, 98%), *N*-hydroxysuccinimide (NHS, 98%), α-bromoisobutyric acid (BIBA, 98%), 2-(dimethylamino)ethyl methacrylate (DMAEMA, >98%), 2,2′-byridine (Bpy, 99%), and copper(I) bromide (CuBr, 99%) were obtained from Sigma-Aldrich Chemical Co., St. Louis, MO. DMAEMA was used after removal of the inhibitors in a ready-to-use disposable inhibitor-removal column (Sigma-Aldrich). 3-(4,5-Dimethylthiazol-2yl)-2,5-diphenyl tetrazolium bromide (MTT), penicillin, and streptomycin were purchased from Sigma Chemical Co., St. Louis, MO. COS7 and HepG2 cell lines were purchased from the American Type Culture Collection (ATCC, Rockville, MD).

Immobilization of ATRP Initiators. The Mg−Al LDH nanoparticles were synthesized using the same procedures as those described earlier.[8,9] As shown in Scheme 1, the immobilization of the ATRP initiators on LDH nanoparticles was carried out in three steps: (1) modification of the LDH surface by 3-(glycidoxypropyl)triethoxysilane (GPTS)[17,22] to produce the LDH surface with terminal epoxide groups (LDH-EX), (2) reaction of the epoxide groups of the LDH-EX nanoparticle with the amine groups of cystamine to attachthe disulfide bonds onto LDH-NH_2, and (3) reaction of the amine groups of LDH-NH_2 with α-bromoisobutyric acid (BIBA) in the presence of EDAC and NHS to produce the 2-bromoisobutyryl-immobilized nanoparticles (LDH-Br).

The silanization process of LDH-EX was performed by adopting similar procedures reported earlier.[19] GPTS, 0.25 mL, was added into an aqueous ethanol solution consisting of 45 mL of alcohol and 5 mL of water, and the solution was stirred for 30 min; 0.5 g of Mg−Al LDH was added, and the resultant reaction mixture was stirred for 6 h. Triethylamine (TEA, 0.25 mL) was added, and the reaction mixture was stirred for another 12 h at room temperature. The resultant LDH-EX nanoparticles were separated by centrifugation, washed exhaustively with copious amounts of ethanol, and then cured at 130 °C to strengthen the silane coating by formation of a polysiloxane network structure. Then, 10 mL of DMSO solution containing cystamine dihydrochloride (1.5 g) and triethyleneamine (TEA, 1.5 mL) was added dropwise into the silanized LDH-EX solution. The reaction mixture was stirred at room temperature under an argon atmosphere for 48 h to produce LDH-NH_2, which was washed exhaustively with copious amounts of deionized water, prior to lyophilization.

The resultant LDH-Br was synthesized via the reaction of the primary groups of LDH-NH_2 with BIBA in the presence of EDAC and NHS. BIBA (0.78 g, 4.5 mmol), EDAC (0.91 g, 4.8 mmol), and NHS (0.75 g, 4.8 mmol) were dissolved in 10 mL of DMSO, and then 1 mL of TEA was added. The mixture was stirred at 37 °C for 2 h and mixed with 0.7 g of LDH-NH_2 dispersed in 10 mL of DMSO. TEA (0.5 mL) was then added, and the reaction mixture was stirred for 48 h at 37 °C. The resultant LDH-Br was washed exhaustively with copious amounts of deionized water, prior to lyophilization.

Synthesis of P(DMAEMA)-Grafted LDH Nanohybrids. For the preparation of LDH-*g*-P(DMEAMA) (LDH-PD) hybrids via ATRP, the molar feed ratio [DMAEMA (2 mL)]/[CuBr]/[Bpy] of 100:1:2.5 was used at room temperature in 5 mL of methanol/water (2/3, v/v) containing 0.1 g of LDH-Br. The reaction was performed in a 25-mL flask equipped with a magnetic stirrer and under the typical conditions for ATRP.[23,24] DMAEMA, LDH-Br, and Bpy were introduced into the flask containing 5 mL of methanol/water, and the reaction mixture was degassed by bubbling argon for 10 min. Then, CuBr was added into the mixture under an argon atmosphere. The flask was then sealed with a rubber stopper under an argon atmosphere. The polymerization was allowed to proceed under continuous stirring at room temperature from 10 to 60 min. The reaction was stopped by diluting with water. The diluted reaction mixture was extensively dialyzed against DDW using a dialysis membrane (MWCO 3500) prior to lyophilization. The LDH-PD yields from ATRP time of 10, 30, and 60 min are 0.12, 0.18, and 0.21 g, respectively.

Hybrid Characterization. The LDH-PD nanoparticles were characterized by X-ray photoelectron spectroscopy (XPS), thermal gravimetric analysis (TGA), scanning electronic microscopy (SEM), and transmission electron microscopy (TEM), respectively. The XPS measurements were performed on a Kratos AXIS HSi spectrometer using a monochromatized Al Kα X-ray source (1486.6 eV photons) and procedures similar to those described earlier.[24] The amount of grafted P(DMAEMA) on LDH was determined by thermal gravimetric analysis (TGA) using a Q50 thermogravimetric analyzer (TA Instruments, Delaware, U.S.A.). The TGA measurements were carried out in

dx.doi.org/10.1021/bc300683y | *Bioconjugate Chem.* 2013, 24, 968−978

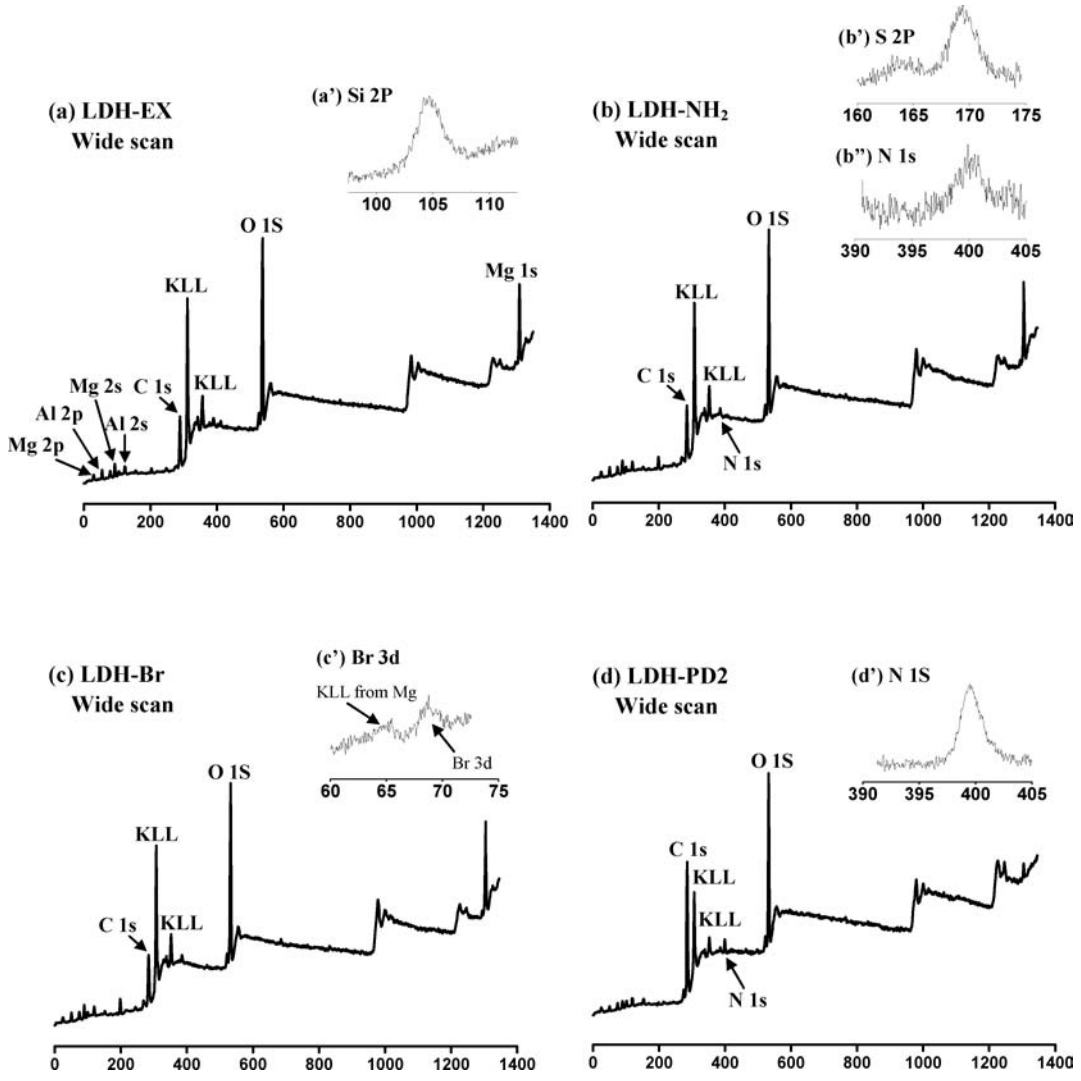

Figure 1. XPS wide-scan spectra of (a) LDH-EX, (b) LDH-NH2, (c) LDH-Br, and (d) LDH-PD2, (a′) Si 2p core-level spectrum of LDH-EX, (b′) S 2p and (b″) N 1s core-level spectra of LDH-NH2, and (c′) Br 3d core-level spectrum of LDH-Br.

air from room temperature to 800 °C at a rate of 5 °C/min. The LDH-PD nanoparticles were also observed with TEM (JEOL JEM 2010F) and SEM (JSM model 6300 SEM, JEOL). For TEM observation, in a typical experiment, one drop of the nanoparticle dispersion was introduced onto a copper grid with the microgrid carbon film. The droplet was allowed to dry under reduced pressure and then observed under TEM operating at an acceleration voltage of 200 kV. For SEM, nanoparticles were dripped on super flat silicon wafers and dried under reduced pressure. The molecular weights of grafted P(DMAEMA) cleaved via HCl etching were determined by gel permeation chromatography (GPC). GPC measurements were performed on a YL9100 GPC system equipped with a UV/vis detector and two 7.8 mm × 300 mm columns of Waters Ultrahydrogel 250 and Ultrahydrogel Linear. Monodispersed poly(ethylene glycol) standards were used to obtain a calibration curve.

Characterization of Hybrid/pDNA Complexes. The plasmid (encoding *Renilla* luciferase) mainly used in this work was pRL-CMV (Promega Co., Cergy Pontoise, France), which was cloned originally from the marine organism *Renilla reniformis*. The plasmid DNA (pDNA) was amplified in *Escherichia coli* and purified according to the supplier's protocol (Qiagen GmbH, Hilden, Germany). The purity and concentration of the purified

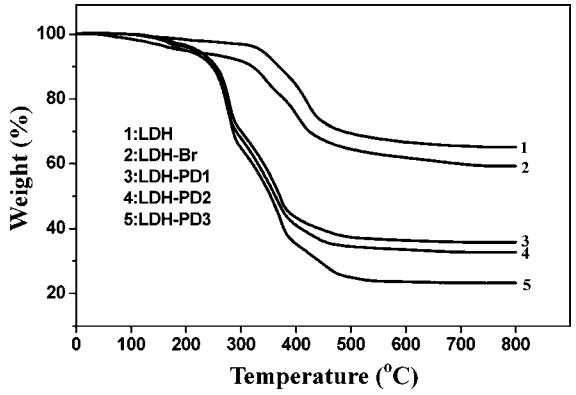

Figure 2. Thermogravimetric analysis of LDH, LDH-Br, and LDH-PDs.

DNA were determined by absorption at 260 and 280 nm and by agrose gel electrophoresis. The purified pDNA was resuspended in Tris-EDTA (TE) buffer and kept in aliquots of 0.5 mg/mL in concentration. All polymer stock solutions were prepared at a nitrogen concentration of 10 mM in distilled water. Solutions were filtered via sterile membranes (0.2 μm) of average pore size and

dx.doi.org/10.1021/bc300683y | *Bioconjugate Chem.* 2013, 24, 968−978

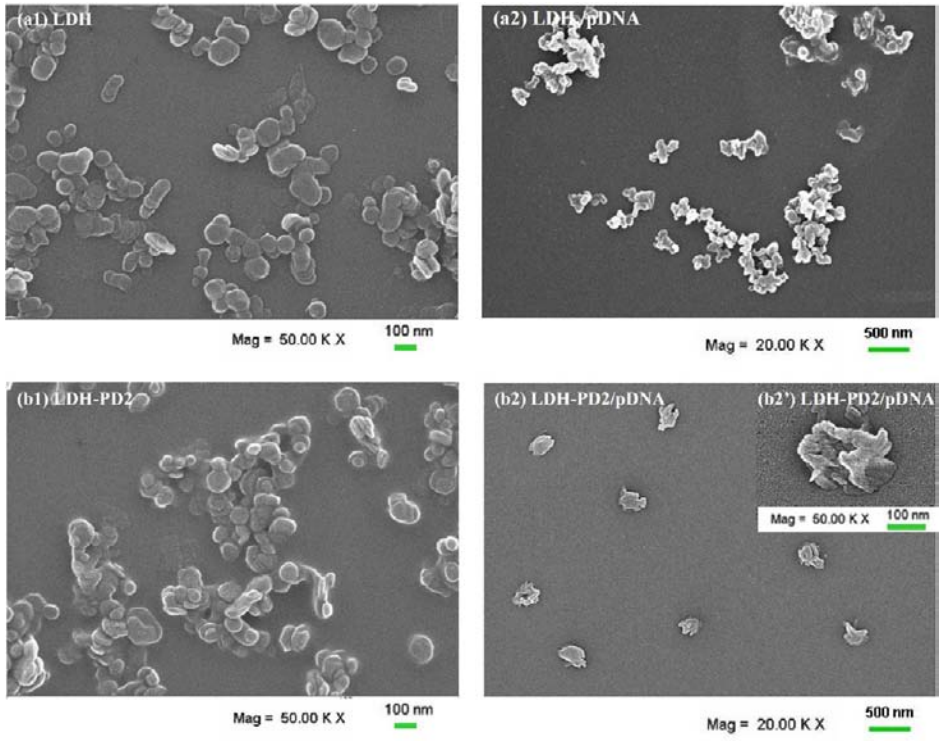

Figure 3. SEM images of (a1) LDH, (a2) LDH/pDNA (at the wt/wt ratio of 10) and (b1) LDH-PD2, (b2) LDH-PD2/pDNA (at the N/P ratio of 5).

stored at 4 °C. Hybrid-to-DNA ratios are expressed as molar ratios of nitrogen (N) in LDH-PDs to phosphate (P) in DNA (or as N/P ratios). The average mass weight of 325 per phosphate group of DNA was assumed. All hybrid/pDNA complexes were formed by mixing equal volumes of polymer and pDNA solutions to achieve the desired N/P ratio. Each mixture was vortexed and incubated for 30 min at room temperature.

Each polymer−LDH hybrid was examined for its ability to bind pDNA through agarose gel electrophoresis using the similar procedures as those described earlier.[25] The hybrid/pDNA complexes at various N/P ratios were investigated. Gel electrophoresis was carried out in TAE running buffer (40 mM Tris-acetate, 1 mM EDTA) with a voltage of 110 V for 30 min in a Sub-Cell system (Bio-Rad Lab, Hercules, CA) such as those previously described.[25] DNA bands were visualized and photographed by a UV trans-illuminator and BioDco-It imaging system (UVP Inc., Upland, CA). The particle sizes and zeta potentials of the polymer/pDNA complexes were measured using a Zetasizer Nano ZS (Malvern Instruments, Southborough, MA, U.S.A.).[25] The polymer/pDNA complexes were also observed with TEM and SEM using the similar procedures as described above.

Cell Viability. The cytotoxicity of the polymer−LDH hybrid was first evaluated using the MTT assay in COS7 and HepG2 cell lines. They were cultured in Dulbecco's Modified Eagle Medium (DMEM), supplemented with 10% heat-inactivated fetal bovine serum (FBS), 100 units/mL of penicillin and 100 μg/mL of streptomycin at 37 °C, under 5% CO_2, and 95% relative humidity atmosphere. The cells were seeded in a 96-well microtiter plate at a density of 10^4 cells/well and incubated in 100 μL of DMEM/well for 24 h. The culture media were replaced with fresh culture media containing serial dilutions of hybrids, and the cells were incubated for 24 h. Then, 10 μL of sterile-filtered MTT stock solution in PBS (5 mg/mL) was added to each well, reaching a final MTT concentration of 0.5 mg/mL. After 5 h, the unreacted dye was removed by aspiration. The produced formazan crystals were dissolved in DMSO (100 μL/well). The absorbance was measured using a Bio-Rad model 680 microplate reader (UK) at a wavelength of 570 nm. The cell viability (%), relative to that of control cells cultured in media without polymers, was calculated from $[A]_{test}/[A]_{control} \times 100\%$, where $[A]_{test}$ and $[A]_{control}$ are the absorbance values of the wells (with the polyplex) and control wells (without the polymers), respectively. For each sample, the final absorbance was the average of those measured from six wells in parallel.

Transfection Assay. Transfection assays were performed first using plasmid pRL-CMV as the reporter gene in COS7 and HepG2 cell lines in the presence of serum. In brief, the cells were seeded in 24-well plates at a density of 5×10^4 cells in 500 μL of medium/well and incubated for 24 h. The hybrid/pDNA complexes (20 μL/well containing 1.0 μg of pDNA) at various N/P ratios were prepared by adding the polymer−LDH hybrid into the DNA solutions, followed by vortexing and incubation for 30 min at room temperature. At the time of transfection, the medium in each well was replaced with 300 μL of fresh normal medium (supplemented with 10% FBS). The complexes were added into the transfection medium and incubated with the cells for 4 h under standard incubator conditions. Then, the medium was replaced with 500 μL of the fresh normal medium (supplemented with 10% FBS). The cells were further incubated for an additional 20 h under the same conditions, resulting in a total transfection time of 24 h. The cultured cells were washed with PBS twice and lysed in 100 μL of the cell culture lysis reagent (Promega Co., Cergy Pontoise, France). Luciferase gene expression was quantified using a commercial kit (Promega Co., Cergy Pontoise, France) and a luminometer (Berthold Lumat LB 9507, Berthold Technologies GmbH & Co. KG, Bad Wildbad, Germany). Protein concentration in the cell samples was analyzed using a bicinchoninic acid

dx.doi.org/10.1021/bc300683y | Bioconjugate Chem. 2013, 24, 968−978

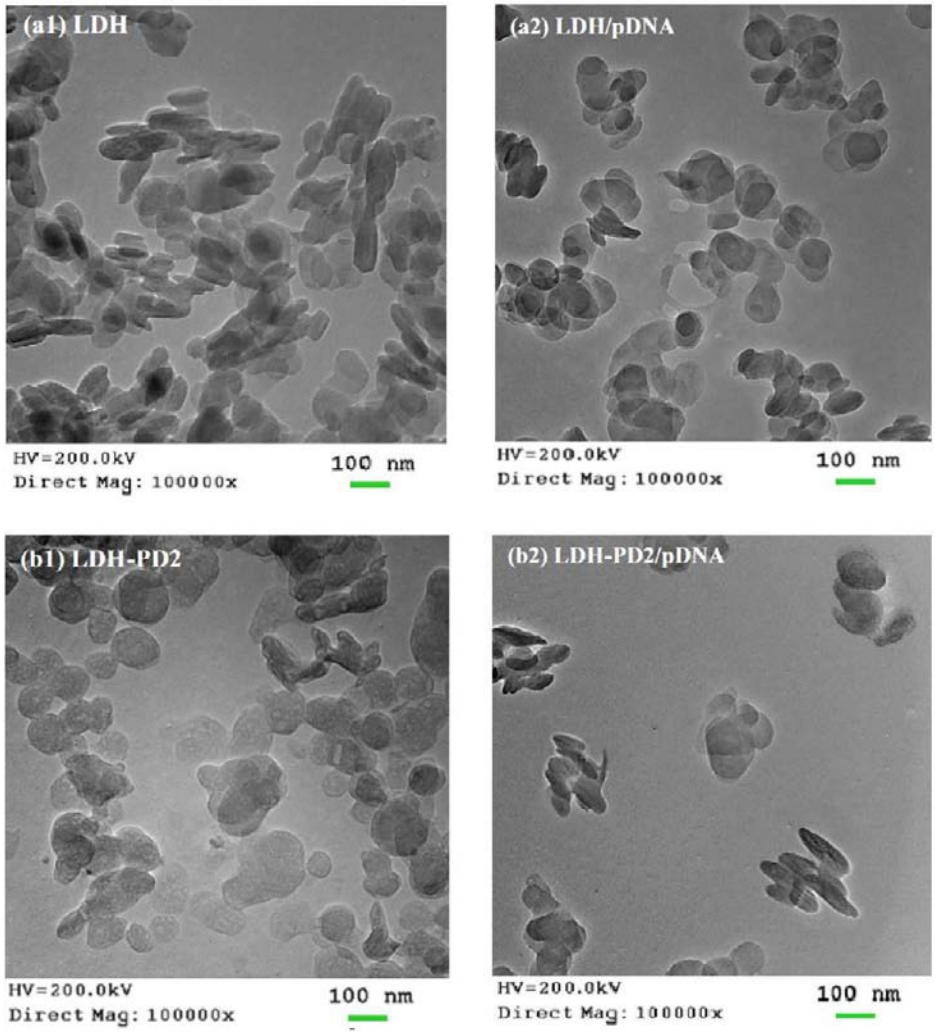

Figure 4. TEM images of (a1) LDH, (a2) LDH/pDNA (at the wt/wt ratio of 10) and (b1) LDH-PD2, (b2) LDH-PD2/pDNA (at the N/P ratio of 5).

assay (Biorad Lab, Hercules, CA, U.S.A.). Gene expression results were expressed as relative light units (RLUs) per milligram of cell protein lysate (RLU/mg protein). LDH-PD-mediated gene transfection was also assessed at their optimal N/P ratios using the enhanced green fluorescent protein (EGFP) pDNA (BD Biosciences, San Jose, CA, U.S.A.) as the reporter gene in HepG2 cell lines using the same procedures as those described above. The transfected cells were imaged by using a Leica DMIL fluorescence microscope. The percentage of the EGFP-positive cells was determined using flow cytometry (FCM, Beckman Coulter, U.S.A.).[26]

Determination of Cellular Internalization. Cells were seeded into a 6-well plate at a density of 4×10^5 cells per well and incubated for 24 h. Then the medium was replaced with 2 mL DMEM without antibiotics. pDNA(pRL-CMV) was labeled with fluorescent dye YOYO-1 in the following way:[27] 1 mmol/L YOYO-1 was diluted 1:100 in PBS. Then 10 μg of pDNA was mixed with 10 μL YOYO-1 dilution (1 molecule of YOYO-1 per 152 base pairs of pDNA) and incubated for 2 h in the dark. Preparation of hybrid/labeled DNA complexes and transfection were performed as described above. The complex containing 6 μg of DNA was applied to each well. The plate was further incubated for 4 h, and then the transfected cells were imaged by using a Leica DMIL fluorescence microscope. For flow cytometry study, the cells were washed with cold PBS, trypsinized, and harvested. Then, the fluorescence intensity and distribution of the cells were measured by flow cytometry (BD FACSAriaII).

RESULTS AND DISCUSSION

Immobilization of ATRP Initiators. For surface-initiated ATRP, it is essential to introduce alkyl halide onto the LDH surface. The LDH surface can be modified covalently by silane, where the siloxane bond is formed between the −OH group of LDH and EtO−Si of silane.[17,22] In this work, as shown in Scheme 1, the LDH surface was first modified with GPTS to produce the LDH surface with terminal epoxide groups (LDH-EX). The epoxide groups of LDH-EX were reacted with the primary amine groups of cystamine to produce the disulfide bonds-containing LDH (LDH-NH_2). Disulfide linkage(s) are easily intracellular reversible, and vectors containing disulfide bonds were already proven to be a highly advantageous feature for delivering a variety of nucleic acids.[28,29] Then, the remaining primary amine groups of LDH-NH_2 were activated to react with α-bromoisobutyric acid (BIBA) in the presence of 1-ethyl-3-(3-dimethylaminopropyl)carbodiimide hydrochloride (EDAC) and *N*-hydroxysuccinimide (NHS), producing the bromoisobutylryl-terminated LDH (LDH-Br). The carboxylic acid groups of BIBA were first converted into reactive esters (succinimidyl intermediates) in the presence of EDAC and

dx.doi.org/10.1021/bc300683y | *Bioconjugate Chem.* 2013, 24, 968−978

NHS. The reactive esters underwent nucleophilic substitution reactions with the primary amine groups to form a stable amide linkage and produce the resultant bromoisobutyryl-terminated LDH-Br as the multifunctional initiator for subsequent ATRP.

Figure 1 shows the X-ray photoelectron spectroscopy (XPS) wide-scan spectra of (a) LDH-EX, (b) LDH-NH_2, and (c) LDH-Br. The elemental peaks were dominated by Al and Mg of LDH.[11,30] The Si 2p (at the binding energy (BE) of about 99 eV[31]) signals are shown in Figure 2a′. The S 2p (with BE at about 164 eV) and N 1s (with BE at about 399 eV) core-level spectra of LDH-NH_2 are shown in Figure 2b′ and b″, respectively. For the LDH-Br surface, the appearance of the Br 3d signal at BE of about 69 eV[31] (characteristic of covalently bonded bromine, Figure 2b′) confirmed that the alkyl halide group has been successfully introduced onto the LDH surface.

Author: The immobilized amount of ATRP initiator of LDH-Br was determined by thermal gravimetric analysis (TGA). Figure 2 shows the TGA results of the LDH-based samples as a function of temperature. The pristine LDH sample shows two general regions of mass loss. Before 350 °C, the slight weight loss was due to the desorption of physisorbed and interlayer water molecules.[30] The loss in the range of 350−550 °C corresponds to the dehydroxylation of the lattices and decomposition of the interlayer anions. On the bases of the weight loss difference (of about 5.8% between LDH and LDH-Br) and surface area (of about 83 m^2/g of LDH determined by the BET method[14]), the surface density of ATRP initiator of LDH-Br was estimated to be about 1.3 initiators/nm^2.

Synthesis of LDH-PD Hybrids. Well-defined LDH-*g*-P(DMEAMA) (LDH-PD) hybrids were subsequently synthesized via ATRP of DMAEMA from LDH-Br (Scheme 1). The LDH-PDs with different molecular weights of P(DMAEMA) brushes can be synthesized by varying the ATRP time. The grafted P(DMEAMA) was cleaved via HCl etching at 50 °C for the gel permeation chromatography (GPC) assay. LDH species were entirely degradable at acidic pH.[7] The number-average molecular weight (M_n) values of the grafted P(DMEAMA) chains of LDH-PD1 (from 10 min of ATRP), LDH-PD2 (from 30 min of ATRP) and LDH-PD3 (from 60 min of ATRP) were 2.0×10^4, 2.3×10^4, and 3.6×10^4 g/mol, respectively. The polydispersity index of P(DMEAMA) is around 1.59. In comparison with the weight loss of LDH-Br, LDH-PD1, LDH-PD2, and LDH-PD3 showed increasing differences in the weight loss (Figure 2). On the basis of the TGA data, the P(DMEAMA) contents in LDH-PD1, LDH-PD2, and LDH-PD3 were 45.1%, 49.9%, and 64.3%, respectively. Figure 1d shows the XPS wide-scan spectrum of LDH-PD2. In comparison with those of LDH-Br (Figure 1c), the Al and Mg signals (associated with the internal LDH parts) of LDH-PD2 decreased substantially. Instead, the strong C and N signals (associated with the grafted P(DMAEMA) chains) were observed. The morphologies of LDH and LDH-PD2 revealed by SEM and TEM were shown in Figure 3a1 and Figure 4a1, respectively. In comparison with LDH, LDH-PD2 exhibited larger particle sizes, indicating that the LDH parts of LDH-PD were wrapped by polymers. The above results indicated that LDH could be readily functionalized via surface-initiated ATRP of P(DMAEMA).

Biophysical Characterization of Hybrid/pDNA Complexes. The DNA condensation capability is a prerequisite for polymeric gene vectors. In this work, the ability of the polymer−LDH hybrids to condense pDNA into particulate structures was confirmed by agarose gel electrophoresis, particle size, and zeta potential measurements, as well as SEM and TEM. The formation of the hybrid/pDNA complexes was first analyzed by their electrophoretic mobility on an agarose gel at various nitrogen (N)/phosphate (P) (or N/P) ratios. Figure 5 shows the gel

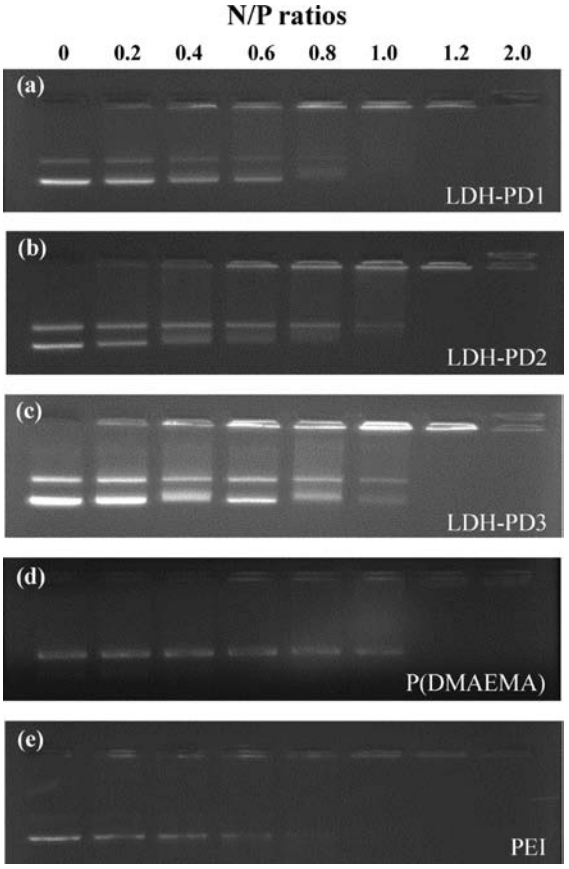

Figure 5. Electrophoretic mobility of pDNA in the complexes of the cationic polymers ((a) LDH-PD1, (b) LDH-PD2, (c) LDH-PD3, (d) P(DMAEMA), and (e) PEI) at various N/P ratios.

retardation results of the LDH-PD/pDNA complexes with increasing N/P ratios, in compared with those of the control P(DMAEMA) homopolymer (with M_n of 2.7×10^4 g/mol[25])/pDNA and branched polyethylenimine (PEI, 25 kDa)/pDNA complexes. All LDH-PDs can compact pDNA completely within the N/P ratio of 1.2, similar to those of the control PDMAEMA and PEI. PEI (25 kDa), one of the most extensively studied nonviral gene vector, is regarded as the gold standard due to its high transfection efficiency in various cell lines.[4,25−27]

The particle size and surface charge of complexes are important factors in modulating their cellular uptake. The (a) particle size and (b) zeta potential of the cationic hybrid/pDNA complexes at various N/P ratios were shown in Figure 6. The hydrodynamic sizes of the pristine LDH-PD nanoparticles were around 200 nm. All the LDH-PD hybrids can efficiently compact pDNA into nanoparticles and showed the decreased particle sizes with the increasing N/P ratios. At the N/P ratio of 2, loose, large aggregates were formed, due to the lower number of cationic hybrids. At higher N/P ratios, all vectors condense pDNA into nanoparticles in the diameter range within 200 nm. These complexes within this size range can readily undergo endocytosis.[32]

Zeta potential, an indicator of surface charges on the hybrid/pDNA nanoparticles, is another important factor affecting cellular uptake of the complexes. A positively charged surface

dx.doi.org/10.1021/bc300683y | Bioconjugate Chem. 2013, 24, 968−978

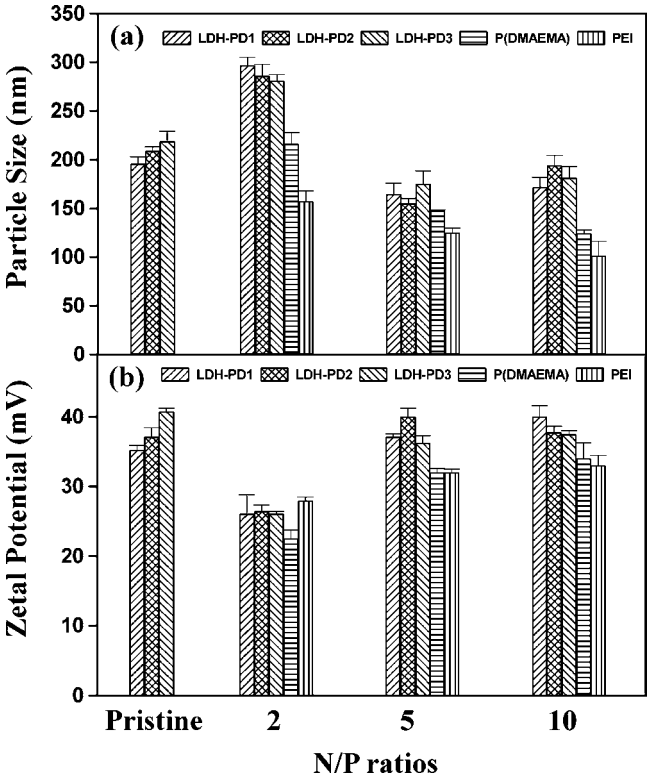

Figure 6. Particle sizes (a) and zeta potentials (b) of the LDH-PD/pDNA, P(DMAEMA)/pDNA, and PEI/pDNA complexes at various N/P ratios in comparison with those of the pristine LDH-PDs. (mean ± SD, n = 3).

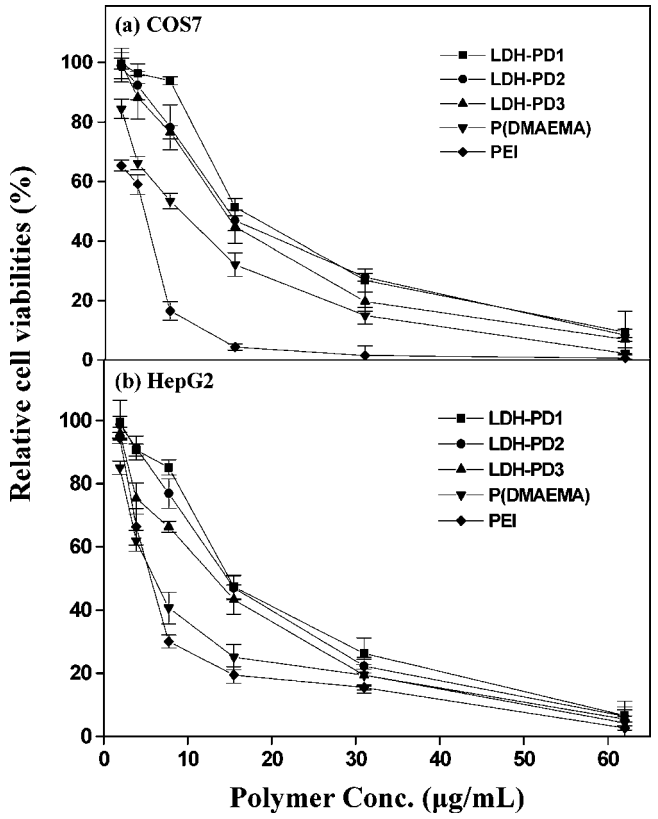

Figure 7. Cell viability assay in (a) COS7 and (b) HepG2 cell lines with various concentrations of LDH-PD1, LDH-PD2, LDH-PD3, P(DMAEMA), and PEI. Cell viability was determined by the MTT assay and expressed as a percentage of the control cell culture.

allows electrostatic interaction with negatively charged cell surfaces and facilitates cellular uptake. As indicated in Figure 6b, the complex surface charge becomes positive upon the complete self-assembly of hybrid and pDNA . At the higher N/P ratios, the LDH-PD/pDNA complexes possessed the excess cationic LDH-PD nanoparticles, which made the particle size and zeta potential of the complexes approach those of the pristine LDH-PD nanoparticles. The positive net surface charge will produce good affinity for anionic cell surfaces.

DNA plasmids could interact with/intercalate into LDH nanoparticles and exhibit an optimal gene delivery efficiency at the weight (w/w) ratio of 10.[10] The typical SEM and TEM images of the LDH/pDNA (at the wt/wt ratio of 10) (a1) and LDH-PD2/pDNA (at a ratio of 5) (b1) complexes are shown in Figure 5 and Figure 6, respectively. In comparison with the loose aggregates of LDH/pDNA, the LDH-PD2/pDNA complexes exist uniformly in the form of compacted nanoparticles, due to the strong electrostatic interaction between the negatively charged DNA and positively charged LDH-PD.

Cell Viability Assay. Cytotoxicity is one important factor to be considered in selecting polymeric gene carriers. Figure 7 shows the in vitro MTT assay results of cytotoxicity of LDH-PD1, LDH-PD2, LDH-PD3, P(DMAEMA), and PEI in (a) COS7 and (b) HepG2 cell cultures. All of the cationic polymers exhibit a dose-dependent cytotoxicity effect.[33] The increased cationic vectors produced the increasing cytotoxicity. The slopes of the dose-dependent cytotoxicity curves for P(DMAEMA) and PEI are much steeper than those for LDH-PDs. In comparison with PEI and P(DMAEMA) homopolymer, the introduction of biocompatible LDH matrix of LDH-PDs not only lowers the cytotoxicity but also imparts biocompatible characteristics to the cationic carriers. These findings are similar to those of our previous studies, where the PDMAEMA side chain conjugated on biocompatible backbones such cellulose,[24] dextran,[26] and chitosan[34] would contribute to the lower cytotoxicity. For LDH-PD hybrids, at the same concentration, the cell viability seems to be highly dependent on the P(DMAEMA) brush length. LDH-PD3 with the longest P(DMAEMA) brushes seems to be the most toxic, both in COS7 and HepG2 cell lines. It is well-known that the cytotoxicity of polycations increases with the molecular weight.[32] Due to the increased length in the P(DMAEMA) brushes of LDH-PD1, LDH-PD2, and LDH-PD3, their cytotoxicity shows the general upward trend as expected. The cytotoxicity of LDH-PDs could be controlled by adjusting the length of the P(DMEAMA) brushes.

In vitro Gene Transfection Assay. The in vitro gene transfection efficiency of the cationic hybrid/pDNA complexes was first assessed using luciferase as a gene reporter in COS7 and HepG2 cell lines. Figure 8 shows the gene transfection efficiencies mediated by LDH-PDs at various N/P ratios in comparison with those of LDH/pDNA (at the optimal weight ratio of 10),[10] P(DMAEMA)/pDNA (at the optimal N/P ratio of 15),[24−26] and PEI (25 kDa, at the optimal N/P ratio of 10).[4,25−27] The transfection efficiency generally first increases at lower N/P ratios and then decreases slightly with the increase in N/P ratios. At lower N/P ratios, pDNA cannot be condensed efficiently by the cationic vectors. At higher N/P ratios, the transfection formulation contains also free vectors. Due to the presence of the increasing amount of free cationic vectors with the increase in N/P ratios, the increasing cytotoxicity may result in a reduction in the transfection efficiency.

dx.doi.org/10.1021/bc300683y | Bioconjugate Chem. 2013, 24, 968−978

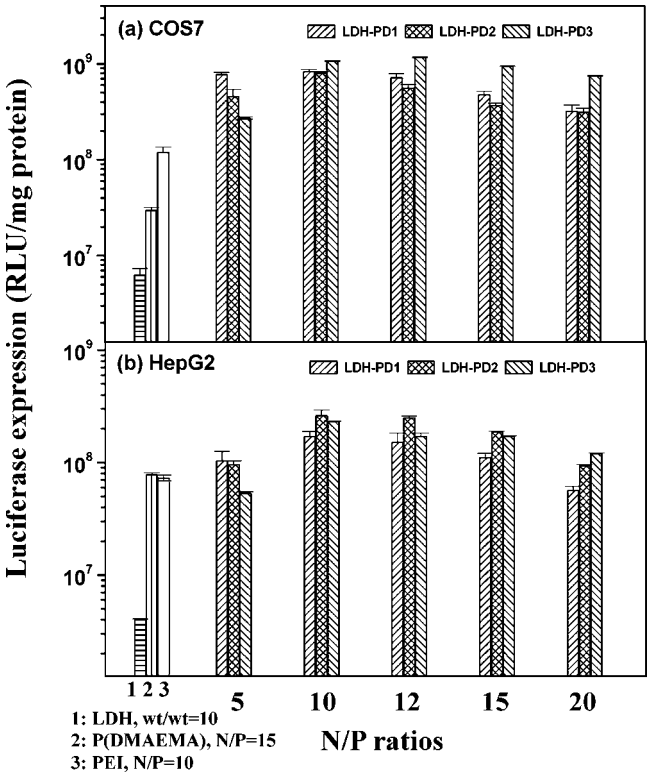

Figure 8. In vitro gene transfection efficiency of the LDH-PD/pDNA complexes at various N/P ratios in comparison with those mediated by LDH (at the optimal weight ratio of 10), P(DMAEMA) (at the optimal N/P ratio of 15), and PEI (25 kDa, at the optimal N/P ratio of 10) in (a) COS7 and (b) HepG2 cell lines.

At most N/P ratios, the transfection efficiencies mediated by LDH-PDs were significantly higher than those mediated by LDH, P(DMAEMA), and PEI at their optimal ratios. In particular, the pristine LDH exhibited very inefficient gene delivery ability. As mentioned above, the molecular weights of grafted P(DMAEMA) chains for LDH-PD1 and LDH-PD2 were respectively 2.0×10^4 and 2.3×10^4 g/mol, not higher than that (2.7×10^4 g/mol) of the control P(DMAEMA) homopolymer.[25] The much better transfection efficiencies mediated by LDH-PD hybrids indicated that the LDH-PD nanoparticles composed of biocompatible LDH species and P(DMAEMA) brushes could substantially enhance gene transfection efficiency. LDH-PD combined the good DNA-condensing ability of P(DMAEMA) and the good biocompatibility and low cytotoxicity of LDH. LDH-based host−guest layered nanoparticles could also interact effectively with some biomolecules.[5−11] The organic/inorganic nanohybrids of LDH-PD could enhance the interaction of the cationic P(DMAEMA) with pDNA or cellular membranes. In addition, for LDH-PD, the P(DMAEMA) chains were linked with LDH via disulfide bridges. The disulfide linkages were responsive to the reductive agent, making P(DMAEMA) chains breakable. Under intracellular reducible conditions, such responsiveness could lead the unstable complexes to greatly facilitate pDNA release from the complexes and benefit the resultant gene expression.[28,29,35]

In an attempt to confirm the gene delivery capability of LDH-PD vectors, direct visualization of gene expression of enhanced green fluorescent protein (EGFP) in HepG2 cells was also performed under fluorescence microscopy. Plasmid pEGFP-N1 encoding GFP was delivered to examine the EGFP

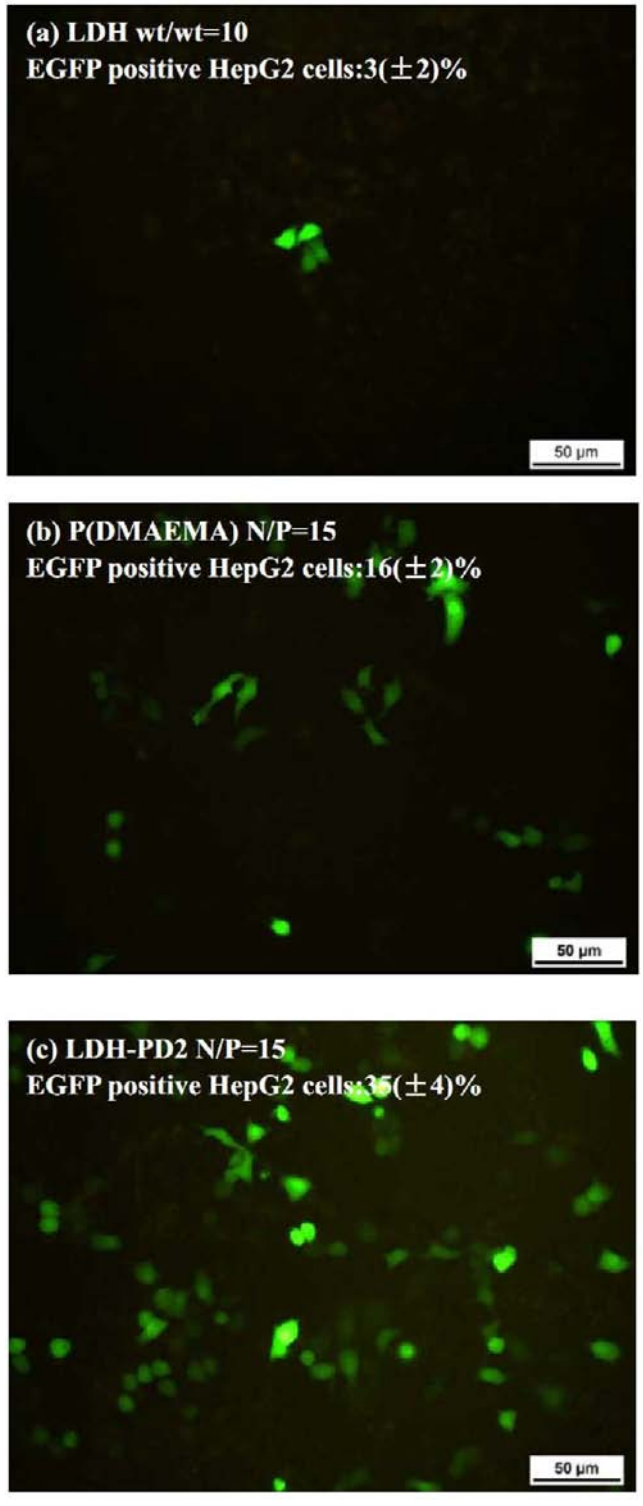

Figure 9. Representative images of EGFP expression mediated by LDH (at the optimal weight ratio of 10), P(DMAEMA) (at the optimal N/P ratios of 15), and LDH-PD2 (at the N/P ratios of 15) in HepG2 cells.

expression. Representative images of EGFP gene expression mediated by LDH, P(DMAEMA), and LDH-PD2 under their optimal conditions are shown in Figure 9. Much stronger fluorescence signals were observed in delivering plasmid EGFP mediated by LDH-PD2 (Figure 9c). In the case of LDH-mediated gene transfection, significantly less fluorescence was

dx.doi.org/10.1021/bc300683y | *Bioconjugate Chem.* 2013, 24, 968−978

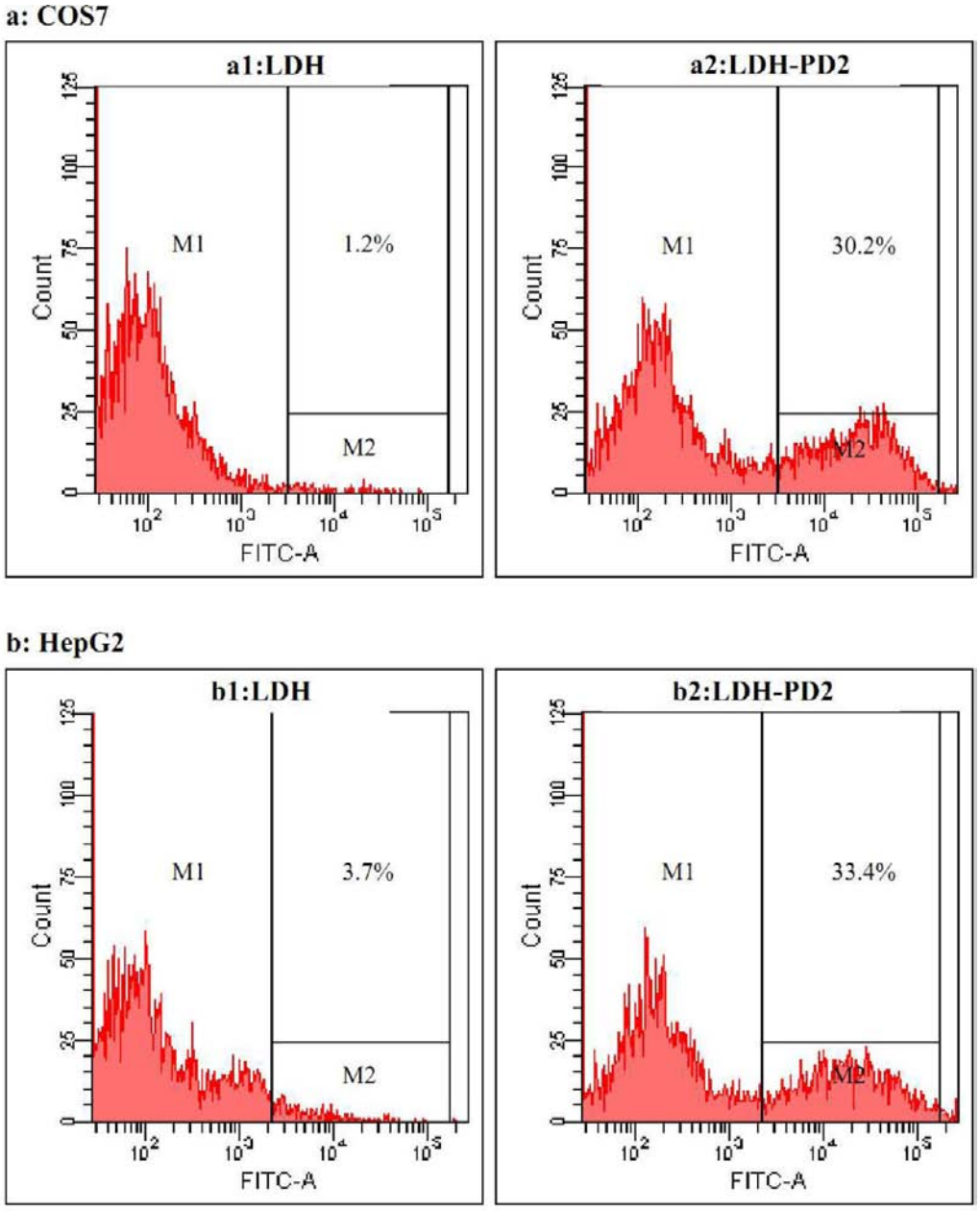

Figure 10. Cellular internalization of the LDH/pDNA (at the wt/wt ratio of 10) and LDH-PD2/pDNA (at the N/P ratio of 15) complexes in (a) COS7 and (b) HepG2 cell lines.

observed in the field of vision (Figure 9a). The transfection efficiency, as reflected by the percentage of the EGFP positive cells, was qualitatively determined using flow cytometry. The percentages of the EGFP-positive cells for LDH, P(DMAEMA), and LDH-PD2 are 3%, 16% and 35%, respectively. The above results were consistent with the results of luciferase expression (Figure 8).

Cellular Internalization. To reveal the influence from P(DMAEMA) brushes, the cellular internalization of the typical LDH/pDNA (at the wt/wt ratio of 10) and LDH-PD2/pDNA (at the N/P ratios of 15) complexes was analyzed by flow cytometry, where pDNA was labeled with YOYO-1 green fluorescent dye. The cellular uptake of the complexes was evaluated by measuring the level of fluorescence associated with the cells. As shown in Figure 10, the LDH-PD2/DNA complex shows the internalization rates of 30.2% in COS7 cells and 33.4% in HepG2 cells, respectively. By contrast, the LDH/DNA complex displays poor cellular association internalization rates of 1.2% in COS7 cells and 3.7% in HepG2 cells, respectively. The above results indicated that the cationic P(DMAEMA) brushes could significantly enhance the cellular uptake of LDH, benefiting the good gene delivery ability of LDH-based vectors.

■ CONCLUSIONS

A flexible three-step method has been successfully developed to introduce the ATRP initiation sites containing disulfide bonds onto LDH surfaces. A series of well-defined cationic LDH-PDs consisting of LDH and disulfide-linked cationic P(DMAEMA) brushes with different lengths were subsequently prepared via ATRP for highly efficient gene delivery. The resultant LDH-PD hybrids were successfully characterized by XPS, TGA, TEM, and SEM. The LD-PDs exhibited good ability to complex

dx.doi.org/10.1021/bc300683y | *Bioconjugate Chem.* 2013, 24, 968−978

pDNA, suitable particle size, and zeta potential for gene transfection. In comparison the poor transfection efficiency of the pristine LDH particles, the LDH-PDs exhibited much higher levels to delivery genes in different cell lines. Moreover, the cationic P(DMAEMA) brushes could also significantly enhance the cellular uptake of LDH. With the versatility of ATRP, properly grafting polycation chains from bioinorganic LDH nanoparticle surfaces is an effective design to produce new LDH-based gene delivery systems.

AUTHOR INFORMATION

Corresponding Author

*E-mail: xufj@mail.buct.edu.cn

Notes

The authors declare no competing financial interest.

ACKNOWLEDGMENTS

This work was supported by National Natural Science Foundation of China (Grants 21074007, 51173014, and 51221002), Research Fund for the Doctoral Program of Higher Education of China (Project No. 20090010120007), Program for New Century Excellent Talents in University (NCET-10-0203), SRF for ROCS, SEM and National High Technology Development Program of China (863 Program 2011AA030102).

REFERENCES

(1) De Smedt, S. C., Demeester, J., and Hennink, W. E. (2000) Cationic polymer based gene delivery systems. *Pharm. Res. 17*, 113−126.

(2) Yudovin-Farber, I., and Domb, A. J. (2007) Cationic polysaccharides for gene delivery. *Mater. Sci. Eng., C 27*, 595−598.

(3) Gu, J. L., Su, S. S., Zhu, M. J., Li, Y. S., Zhao, W. R., Duan, Y. R., and Shi, J. L. (2012) Targeted doxorubicin delivery to liver cancer cells by PEGylated mesoporous silica nanoparticles with a pH-dependent release profile. *Microporous Mesoporous Mater. 161*, 160−167.

(4) Cai, Q., Zhu, Y., He, J. Q., Wang, Z. H., Xu, F. J., Yang, X. P., and Yang, W. T. (2012) Well-defined hydroxyapatite−polycation nanohybrids via surface-initiated atom transfer radical polymerization for biomedical applications. *J. Mater. Chem. 22*, 9358−9367.

(5) Choy, J. H., Jung, J. S., Oh, J. M., Park, M., Jeong, J., Kang, Y. K., and Han, O. J. (2004) Layered double hydroxide as an efficient drug reservoir for folate derivatives. *Biomaterials 25*, 3059−3064.

(6) Desigaux, L., Belkacem, M. B., Richard, P., Cellier, J., Leone, P., Cario, L., Leroux, F., Taviot-Gueho, C., and Pitard, B. (2006) Self-assembly and characterization of layered double hydroxide/DNA hybrids. *Nano Lett. 6*, 199−204.

(7) Gu, Z., Thomas, A. C., Xu, Z. P., Campbell, J. H., and Lu, G. Q. (2008) In vitro sustained release of LMWH from Mg Al-layered double hydroxide nanohybrids. *Chem. Mater. 20*, 3715−3722.

(8) Zhang, H., Pan, D., and Duan, X. (2009) Synthesis, characterization, and magnetically controlled release behavior of novel core−shell structural magnetic ibuprofen-intercalated LDH nanohybrids. *J. Phys. Chem. C 113*, 12140−12148.

(9) Pan, D., Zhang, H., Zhang, T., and Duan, X. (2010) A novel organic−inorganic microhybrids containing anticancer agent doxifluridine and layered double hydroxides: Structure and controlled release properties. *Chem. Eng. Sci. 65*, 3762−3771.

(10) Ladewig, K., Niebert, M., Xu, Z. P., Gray, P. P., and Lu, G. Q. (2010) Controlled preparation of layered double hydroxide nanoparticles and their application as gene delivery vehicles. *Appl. Clay Sci. 48*, 280−289.

(11) Hu, H., Wang, X. B., Xu, S. L., Yang, W. T., Xu, F. J., Shen, J., and Mao, C. (2012) Preparation and evaluation of well-defined hemocompatible layered double hydroxide-poly(sulfobetaine) nanohybrids. *J. Mater. Chem. 22*, 15362−15369.

(12) Layered double hydroxide: Synthesis and postsynthesis modifications. In *Layered Double Hydroxides: Present and Future*. (Rives, V., Ed.) Nova Science Publishers: New York, (2001).

(13) Nalawade, P., Aware, B., Kadam, V. J., and Hirlekar, R. S. (2009) Layered double hydroxides: A review. *J. Sci. Ind. Res 68*, 267−272.

(14) Wang, B., Zhang, H., Evans, D. G., and Duan, X. (2005) Surface modification of layered double hydroxides and incorporation of hydrophobic organic compounds. *Mater. Chem. Phys. 92*, 190−196.

(15) Park, A. Y., Kwon, H., Woo, A. J., and Kim, S. J. (2005) Layered double hydroxide surface modified with (3-aminopropyl)-triethoxysilane by covalent bonding. *Adv. Mater. 17*, 106−109.

(16) Qiu, L., Chen, W., and Qu, B. (2005) Exfoliation of layered double hydroxide in polystyrene by in-situ atom transfer radical polymerization using initiator-modified precursor. *Colloid Polym. Sci. 283*, 1241−1245.

(17) Oh, J. M., Choi, S. J., Lee, G. E., Han, S. H., and Choy, J. H. (2009) Inorganic drug-delivery nanovehicle conjugated with cancer-cell-specific ligand. *Adv. Funct. Mater. 19*, 1617−1624.

(18) Amiji, M., and Paik, K. (1993) Surface modification of polymeric biomaterials with poly(ethylene oxide): Albumin and heparin for reduced thrombogenicity. *J. Biomater. Sci. Polymer Edn. 4*, 217−234.

(19) Xu, F. J., Neoh, K. G., and Kang, E. T. (2009) Bioactive surfaces and biomaterials via atom transfer radical polymerization. *Prog. Polym. Sci. 34*, 719−761.

(20) Xu, F. J., and Yang, W. T. (2011) Polymer vectors via controlled/living radical polymerization for gene delivery. *Prog. Polym. Sci. 36*, 1099−1131.

(21) Matyjaszewski, K., and Xia, J. H. (2001) Atom transfer radical polymerization. *Chem. Rev. 101*, 2921−2990.

(22) Wei, J., Liu, A., Chen, L., Zhang, P., Chen, X., and Jing, X. (2009) The surface modification of hydroxyapatite nanoparticles by the ring opening polymerization of γ-benzyl-L-glutamate *N*-carboxyanhydride. *Macromol. Biosci. 9*, 631−638.

(23) Xu, F. J., Zhu, Y., Liu, F. S., Nie, J., Ma, J., and Yang, W. T. (2010) Comb-shaped conjugates comprising hydroxypropyl cellulose backbones and low-molecular-weight poly(*N*-isopropylacryamide) side chains for smart hydrogels: Synthesis, characterization and biomedical applications. *Bioconjugate Chem. 21*, 456−464.

(24) Xu, F. J., Ping, Y., Ma, J., Tang, G. P., Yang, W. T., Kang, E. T., and Neoh, K. G. (2009) Comb-shaped copolymers composed of hydroxypropyl cellulose backbones and cationic poly((2-dimethylamino)ethyl methacrylate) side chains for gene delivery. *Bioconjugate Chem. 20*, 1449−1458.

(25) Xu, F. J., Li, H. Z., Li, J., Zhang, Z. X., Kang, E. T., and Neoh, K. G. (2008) Pentablock copolymers of poly(ethylene glycol), poly((2-dimethyl amino)ethyl methacrylate) and poly(2-hydroxyethyl methacrylate) from consecutive atom transfer radical polymerizations for non-viral gene delivery. *Biomaterials 29*, 3023−3033.

(26) Wang, Z. H., Li, W. B., Ma, J., Tang, G. P., Yang, W. T., and Xu, F. J. (2011) Functionalized nonionic dextran backbones by atom transfer radical polymerization for efficient gene delivery. *Macromolecules 44*, 230−239.

(27) Dai, F. Y., and Liu, W. G. (2011) Enhanced gene transfection and serum stability of polyplexes by PDMAEMA-polysulfobetaine diblock copolymers. *Biomaterials 32*, 628−638.

(28) Neu, M., Germershaus, O., Mao, S., Voigt, K. H., Behe, M., and Kissel, T. (2007) Crosslinked nanocarriers based upon poly-(ethyimine) for systemic plasmid delivery: in vitro characterization and in vivo studies in mice. *J. Controlled Release 118*, 370−380.

(29) Manickam, D. S., and Oupicky, D. (2006) Multiblock reducible copolypeptides containing histidine-rich and nuclear localization sequences for gene delivery. *Bioconjugate Chem 17*, 1395−1403.

(30) Li, F., Zhang, L., Evans, D. G., Forano, C., and Duan, X. (2004) Structure and thermal evolution of Mg−Al layered double hydroxide containing interlayer organic glyphosate anions. *Thermochim. Acta 424*, 15−23.

(31) Moulder, J. F., Stickle, W. F., Sobol, P. E., and Bomben, K. D. (1992) In *X-ray Photoelectron Spectroscopy*; (Chastain, J., Ed.) Perkin-Elmer: Eden Prairie, MN.
(32) Wetering, P. V. D., Moret, E. E., Nieuwenbroek, N. M. E., Steenbergen, M. J. V., and Hennink, W. E. (1999) Structure-activity relationship of water-soluble cationic methacrylate/methacrylmide polymers for nonviral gene delivery. *Bioconjugate Chem. 10*, 589−97.
(33) vande Wetering, P., Cherng, J. Y., Talsma, H., and Hennink, W. E. (1997) Relation between transfection efficiency and cytotoxicity of poly(2-(dimethylamino)ethyl methacrylate)/plasmid complexes. *J. Controlled Release 49*, 59−69.
(34) Ping, Y., Liu, C. D., Tang, G. P., Li, J. S., Li, J., Yang, W. T., and Xu, F. J. (2010) Functionalization of chitosan via atom transfer radical polymerization for gene delivery. *Adv. Funct. Mater. 20*, 3106−3116.
(35) Wang, Z. H., Zhu, Y., Chai, M. Y., Yang, W. T., and Xu, F. J. (2012) Biocleavable comb-shaped gene carriers from dextran backbones with bioreducible ATRP initiation sites. *Biomaterials 33*, 1873−1883.